THE JOURNAL OF BIOLOGICAL CHEMISTRY VOL. 289, NO. 45, pp. 31330–31340, November 7, 2014

Gln-362 of Angiopoietin-2 Mediates Migration of Tumor and Endothelial Cells through Association with $\alpha5\beta1$ Integrin

Received for publication, April 21, 2014, and in revised form, September 1, 2014 Published, JBC Papers in Press, September 18, 2014, DOI 10.1074/jbc.M114.572594

Hyo Seon Lee[‡1], Seung Ja Oh[‡1], Kwang-Hoon Lee[‡2], Yoon-Sook Lee[‡], Eun Ko[‡], Kyung Eun Kim[‡], Hyung-chan Kim[‡], Seokkyun Kim[‡], Paul H. Song[‡], Yong-In Kim[§], Chungho Kim[‡¶3], and Sangyeul Han[‡4]

From the [‡]Bio Therapeutics Lab, Samsung Advanced Institute of Technology, Samsung Electronics Co., Ltd., 130 Samsung-ro, Yeongtong-gu, Suwon-si, Gyeonggi-do 443-803, South Korea, the [§]Well Aging Center, Samsung Advanced Institute of Technology, Samsung Electronics Co., Ltd., Suwon-Si 443-803, South Korea, and the [¶]School of Life Sciences and Biotechnology, Korea University, Seoul 136-701, South Korea

Background: The angiogenic growth factor angiopoietin-2 regulates angiogenesis through Tie2 and integrins.
Results: An angiopoietin-2 mutant fails to bind to integrin, but not Tie2, and to mediate cell migration.
Conclusion: Tie2-independent angiopoietin-2 association with integrin is critical for migration of tumor and endothelial cells.
Significance: Understanding the mechanism of angiopoietin-2 interaction with integrin is essential for angiogenesis and cancer invasion.

Angiopoietin-2 (Ang-2) not only regulates angiogenesis by binding to its well known receptor Tie2 on endothelial cells but also controls sprouting of Tie2-negative angiogenic endothelial cells and invasion of Tie2-negative non-endothelial cells by binding to integrins. However, the molecular mechanism of the Ang-2/integrin association has been unclear. In this study, we found that the Gln-362 residue of Ang-2 was essential for binding to $\alpha5\beta1$ integrin. A Q362E Ang-2 mutant, which still bound to Tie2, failed to associate with $\alpha5\beta1$ integrin and was unable to activate the integrin downstream signaling of focal adhesion kinase. In addition, unlike wild-type Ang-2, the Q362E Ang-2 mutant was defective in mediating invasion of Tie2-negative glioma or Tie2-positive endothelial cells. Furthermore, the tailpiece domain of the $\alpha5$ subunit in $\alpha5\beta1$ integrin was critical for binding to Ang-2. Taken together, these results provide a novel insight into the mechanism of integrin regulation by Ang-2, which contributes to tumor invasion and endothelial cell migration in a Tie2-independent manner.

The formation of new blood vessels (angiogenesis) plays a fundamental role in development and tumor growth. Sprouting, growth, and maturation of newly growing vessels are coordinated by an array of proangiogenic growth factors, including vascular endothelial growth factor (VEGF) and angiopoietins, in a spatiotemporal manner (1, 2).

Angiopoietins are critical growth factors that regulate angiogenesis (1, 3, 4). Among them, angiopoietin-2 (Ang-2)[5] plays a proangiogenic role by competing with angiopoietin-1 (Ang-1) for binding to their common receptor, Tie2, a receptor tyrosine kinase specifically expressed in endothelial cells. Ang-1 maintains the vessel integrity by activating Tie2 signaling in mature vasculature, whereas Ang-2 destabilizes endothelial cells and increases vessel sprouting and permeability by antagonizing Ang-1. However, Ang-2 is likely to act as a Tie2 agonist in some contexts, as reported previously in tumor endothelial cells and lymphatic vessels (5, 6), suggesting that Ang-2 may have context-dependent functions.

Notably, Tie2-independent functions of Ang-2 have also been documented in both endothelial and non-endothelial cells. Several reports have suggested that, by directly or indirectly controlling integrins, Ang-2 enhances tumor metastasis and angiogenesis. Ang-2 regulates integrins indirectly by inducing the formation of Tie2/$\alpha v\beta3$ integrin (7) or Tie2/$\alpha5\beta1$ integrin complexes (8, 9). Moreover, Ang-2 interacts directly with $\alpha v\beta1$ and $\alpha5\beta1$ integrins and activates the downstream focal adhesion kinase (FAK), ILK, Akt, and ERK signaling pathways in Tie2-deficent glioma and breast cancer cells (9–11). In endothelial cells, Ang-2 binds to $\alpha v\beta3$, $\alpha5\beta1$, and $\alpha v\beta5$ integrins with lower affinity than Tie2, which activates FAK phosphorylation at Tyr-397 and enhances sprouting and migration of Tie2-negative tip cells (12). However, despite these reports, detailed information about the binding domains that mediate their association is still lacking.

In this study, we investigated the molecular mechanism by which Ang-2 and integrins form a complex. Through systematic screening and mutational analyses, we have demonstrated that the Gln-362 residue of Ang-2, which is not involved in Tie2 binding, is critical for the interaction with $\alpha5\beta1$ integrin. We also tested the ability of the Q362E Ang-2 mutant to regulate cell adhesion and invasion. Furthermore, we identified the tailpiece domain of the $\alpha5$ subunit in $\alpha5\beta1$ integrin as a critical determinant for binding to Ang-2. This study suggests that blockade of Ang-2/integrin interaction by targeting a domain including the Gln-362 residue of Ang-2 could be effective for inhibition of tumor invasion and metastasis.

[1] Both authors contributed equally to this work.
[2] Present address: New Drug Development Center, Osong Medical Innovation Foundation, Cheongju, Chungbuk 363-951, South Korea.
[3] To whom correspondence may be addressed: School of Life Sciences and Biotechnology, Korea University, Seoul 136-701, South Korea. Tel.: 82-2-3290-3402; Fax: 82-2-3290-4144; E-mail: chungho@korea.ac.kr.
[4] To whom correspondence may be addressed. Tel.: 82-31-8061-4533; Fax: 82-31-8061-4666; E-mail: sangyeul.han@samsung.com.
[5] The abbreviations used are: Ang-2, angiopoietin-2; FAK, focal adhesion kinase; Ang-1, angiopoietin-1; HUVECs, human umbilical vein endothelial cells; RBD, receptor-binding domain; IMDM, Iscove's modified Dulbecco's medium.

EXPERIMENTAL PROCEDURES

Cell Lines and Reagents—The U87MG cell line was purchased from the American Type Culture Collection, and the Chinese hamster ovary (CHO) cell line was obtained from the Biological Resource Center at the Korea Research Institute of Bioscience and Biotechnology. Cells were maintained in Iscove's modified Dulbecco's medium (IMDM; Invitrogen) supplemented with 10% fetal bovine serum (FBS), 1% penicillin/streptomycin, and 1% non-essential amino acids. Human umbilical vein endothelial cells (HUVECs) were purchased from Lonza and maintained in endothelial growth medium 2 (Lonza, Walkersville, MD). Lipofectamine 2000 (Invitrogen) was used according to the manufacturer's protocol for transient transfection. Small interference RNA (siRNA) targeting α5 and β1 integrin and control siRNA were purchased from Dharmacon (Lafayette, CO). The following reagents and antibodies were also used: CellTiter-Glo™ reagent (Promega, Madison, WI), anti-FLAG antibody (M2, Sigma-Aldrich), anti-Tie2 antibody (Santa Cruz Biotechnology, Inc.), anti-GAPDH antibody (Cell Signaling Technology, Danvers, MA), anti-phospho-FAK-(Tyr-397) antibody (BIOSOURCE, Camarillo, CA), anti-FAK antibody (Santa Cruz Biotechnology), β1 integrin-blocking antibody (JB1A, Millipore, Billerica, MA), β3 integrin-blocking antibody (B3A, Millipore), poly-L-lysine (Sigma-Aldrich), and fibronectin (Invitrogen). Recombinant proteins, such as Ang-2, Tie2-Fc, and integrin α5β1, were purchased from R&D Systems (Minneapolis, MN).

Plasmids—A human FLAG-Ang-2 cDNA (amino acids 1–496) was synthesized (Bioneer, Daejeon, Korea) and cloned into the pCMV vector (Invitrogen). The Q362E Ang-2 mutant was generated using QuikChange site-directed mutagenesis kit (Agilent Technologies, Inc., Santa Clara, CA). Human α5 and β1 integrin cDNAs were purchased from Origene, and open reading frames of integrins were amplified by PCR and cloned into the pcDNA3.1 vector (Invitrogen). Human Ang-1 cDNA was synthesized (Bioneer) and cloned into the pFLAG-CMV2 vector (Invitrogen). The plasmid encoding 15-peptibody was generated by fusing the DNA sequence of Ang-2 peptide 15 with a Gly-Gly-Gly-Ser linker to the N and C termini of an immunoglobulin Fc fragment in the pFUSE vector (Invitrogen).

Ang-2 Overlapping Peptides—Peptide sequences were derived from the receptor-binding domain (RBD) (amino acids 282–496) of human Ang-2. A total of 41 peptides (15-mers) in which each peptide sequence overlapped with a neighboring peptide by 10 amino acids were chemically synthesized (Peptron, Daejeon, Korea) and reconstituted at 100 mg/ml in DMSO (Sigma). HPLC showed that all peptides were >90% pure.

Purification of FLAG-Ang-2 Proteins and 15-Peptibody—FLAG-Ang-2 and Ang-2 mutants were expressed in HEK293-F cells (Invitrogen) for 4 days at 37 °C and then purified from the cultured medium using anti-FLAG M2 affinity gel (Sigma). The bound FLAG-Ang-2 or Q362E FLAG-Ang-2 proteins were eluted with PBS containing 100 μg/ml 3× FLAG peptide (Sigma). The 15-peptibody was expressed in HEK293-F cells (Invitrogen) for 5 days at 37 °C and then purified from the cultured medium using HiTrap MabSelect SuRe columns (GE Healthcare). The protein was eluted with IgG Elution Buffer (Thermo Scientific, Rockford, IL), neutralized to pH 7.0, and then buffer-exchanged into PBS.

Ang-2-dependent Cell Adhesion—Six-well, 96-well, or multiwell plates (μ-slide 8-well, Ibidi GmbH) were coated with 10 μg/ml Ang-2 (R&D Systems), FLAG-Ang2, or Q362E FLAG-Ang2 in PBS by incubation at 4 °C for 16 h. The wells were washed twice with PBS and treated with PBS containing 2% (v/v) bovine serum albumin (BSA) for 2 h at room temperature for blocking. Empty wells treated with 2% BSA were used as a control. U87MG cells (70–80% confluent) were trypsinized, washed twice, and resuspended in serum-free IMDM. Cell suspensions were added to each well and incubated for 2 h in 37 °C in a CO_2 incubator to allow cell adhesion. The plates were then washed four times with serum-free IMDM to remove unbound cells. Bound cells were quantified by CellTiter-Glo reagent and in an EnVision Multilabel Reader (PerkinElmer Life Sciences). Rhodamine-phalloidin (Molecular Probes, Inc., Carlsbad, CA) and an anti-vinculin antibody (Sigma-Aldrich) were applied for immunostaining. Cells were visualized under a confocal laser-scanning microscope (Carl Zeiss).

For immunoblotting, serum-starved U87MG cells were detached with enzyme-free cell dissociation solution (Invitrogen) and resuspended in serum-free IMDM. Cell suspensions were added to the wild-type or Q362E Ang-2-coated wells and then incubated for the indicated times. The attached cells were collected, and cell lysates were prepared with Complete Lysis-M buffer (Roche Applied Science) containing a protease inhibitor mixture (Roche Applied Science). The protein lysates were subjected to SDS-PAGE and transferred into nitrocellulose membranes. The protein blots were then probed with anti-phospho-FAK(Tyr-397), FAK, and GAPDH antibodies.

ELISA—ELISA plates were coated with 5 μg/ml α5β1 integrin or Tie2 in PBS at 4 °C for 16 h, washed twice with PBS, and then treated with blocking solution (1% BSA in PBS) at room temperature for 2 h. The blocking solution was removed, and the plates were incubated with 10 μg/ml FLAG-Ang-2, Q362E FLAG-Ang2, or fibronectin diluted in blocking solution at room temperature for 2 h. The plates were washed five times with T-PBS (0.1% Triton X-100 in PBS) and then incubated with an anti-FLAG antibody conjugated to horseradish peroxidase (HRP; Sigma) at room temperature for 1 h. After washing five times with T-PBS, the HRP substrate 3,3′,5,5′-tetramethylbenzidine (Cell Signaling) was added to the plates according to the manufacturer's instructions. Reactions were stopped with Stop solution (Cell Signaling), and color development was quantified at 450 nm using a Spectra MAX340 plate reader (Molecular Devices, Sunnyvale, CA).

Flow Cytometric Analysis—The cDNAs encoding various integrins and GFP/pTRACER™-CMV2 (Invitrogen) as a transfection marker were cotransfected into CHO cells at a ratio of 10:1 (integrins/GFP). At 1 day after transfection, the transfected cells were detached by trypsinization and resuspended in IMDM at a concentration of 2×10^7 cells/ml. A cell suspension (45 μl) was mixed with 5 μl of 200 μg/ml FLAG-Ang-2 or Q362E FLAG-Ang-2 and then incubated on ice for 1 h. A formaldehyde solution (4%, v/v) (400 μl) was added directly to the mixture for fixation, followed by three washes with IMDM. The cells were then incubated with an anti-FLAG antibody conjugated to R-phycoerythrin for 1 h,

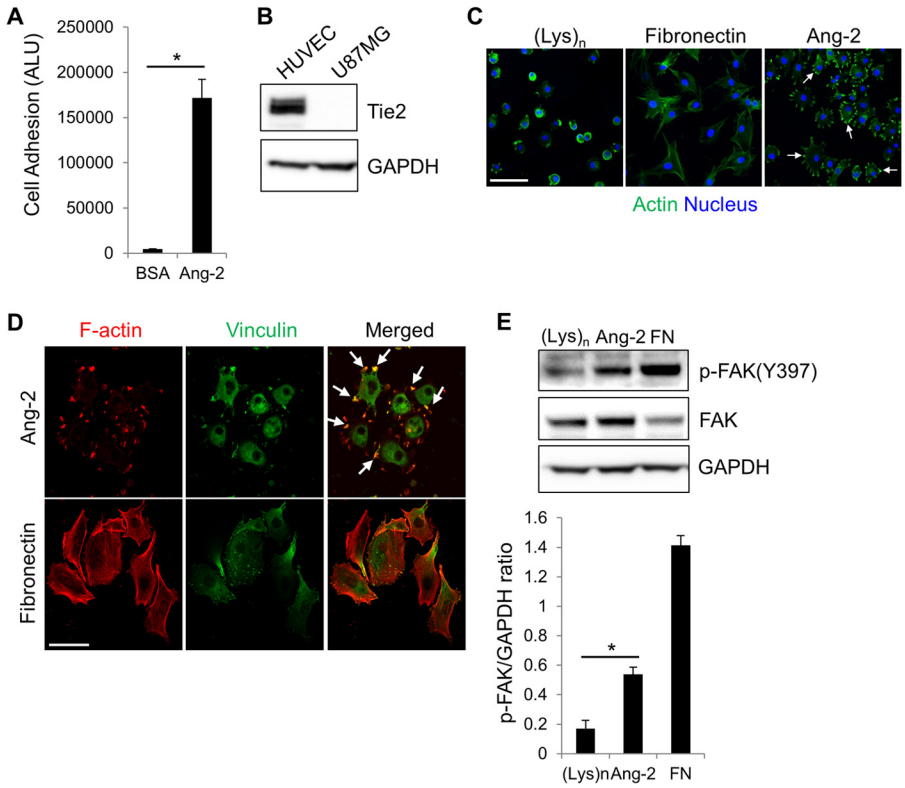

FIGURE 1. **Ang-2-dependent cell adhesion.** *A*, U87MG cells were incubated on an Ang-2-coated plate for 2 h. Bound cells were then quantified using CellTiter-Glo™ reagent. Cells bound to a BSA-coated plate were used as the negative control. The degree of cell adhesion was expressed as arbitrary light units (*ALU*). *Error bars*, S.D. ($n = 3$; *, $p < 0.001$). *B*, expression levels of Tie2 in HUVECs and U87MG cells were examined by Western blot analyses. *C*, representative immunofluorescent staining images of U87MG cells bound to the plates coated with 100 μg/ml poly-L-lysine, 10 μg/ml fibronectin, or 10 μg/ml Ang-2. Bound cells were fixed and then incubated with rhodamine-phalloidin and DAPI to detect actin (*green*) and nuclei (*blue*), respectively. *Arrows*, examples of actin-rich structures. *Scale bar*, 100 μm. *D*, representative immunofluorescent staining images of U87MG cells stained with rhodamine-phalloidin (*red*) and an anti-vinculin antibody (*green*). *Arrows*, examples of actin-rich projections. *Scale bar*, 50 μm. *E*, U87MG cells were seeded on plates coated with 100 μg/ml poly-L-lysine ($(Lys)_n$), 10 μg/ml Ang-2, or 10 μg/ml fibronectin (*FN*). After 1 h, lysates of bound cells were prepared, and phosphorylation of FAK at the Tyr-397 site was examined by Western blot analyses with an anti-phospho-FAK (Tyr-397) (*pFAK (Y397)*) antibody. The graph shows the densitometric analysis of phosphorylated FAK(Tyr-397) levels normalized to GAPDH levels. Data are represented as mean ± S.E. (*error bars*) ($n = 3$; *, $p < 0.01$).

washed twice with IMDM, and analyzed on a FACSCanto II system (BD Biosciences). The expression of GFP as the transfected marker (*y* axis) and the degree of Ang-2 binding (*x* axis) have been depicted in dot plots. The data were imported into MATLAB R2009a software, and the geometric mean values were calculated for Ang-2 binding in cells expressing specific levels of GFP. Mean values have been indicated in dot plots as *larger red dots*. To specifically examine the effect of Ang-2 only in the cell population transfected with exogenous integrins or Tie2, the geometric mean values of the Ang-2 binding degree (*y* axis) in cells expressing different levels of GFP density (*x* axis) were plotted as linear graphs.

Invasion Assay—Invasion assays were performed using Matrigel matrix-coated Fluoroblok™ 24-multiwell invasion plates (8-μm pore size; BD Biosciences). Transwell inserts were additionally coated with 10 μg/ml FLAG-Ang-2 or Q362E FLAG-Ang-2 at 4 °C for 16 h and then incubated with 2% BSA for 1 h at 37 °C for blocking. As a negative control, inserts were coated with BSA instead of Ang-2. Serum-starved cells were detached with an enzyme-free cell dissociation solution (Invitrogen) and resuspended with serum-free medium. U87MG (1×10^5) cells were added to each insert, and the bottom chambers were filled with IMDM containing 2% FBS. For CHO cell and HUVEC invasion assays, 5×10^4 cells were added to each insert, and the bottom chambers were filled with IMDM or EBM-2 containing 1% FBS, respectively. Cells were allowed to invade through the Matrigel at 37 °C for 16 h and then stained with 10 μM calcein-AM (BD Bioscience). For quantification of invasion, the fluorescence intensity was measured using an Envision 2104 multilabel reader (PerkinElmer Life Sciences) with the bottom reading setting at excitation and emission wavelengths of 485 and 535 nm, respectively. Representative images were acquired by microscopy (Carl Zeiss).

Immunofluorescent Staining Analysis—Cells on μ-slide 8-well plates (Ibidi) were fixed with 4% formaldehyde in PBS (pH 7.2), permeabilized with 0.1% Triton X-100, blocked in 1% BSA in PBS, and incubated with primary antibodies at room temperature for 3 h. The cells were incubated with secondary antibodies at room temperature for 1 h and mounted with Vectashield mounting medium with DAPI (Vector Labs). Images were collected on a confocal laser-scanning microscope (Carl Zeiss).

Generation of Integrin Hybrids—Human α5αv and β1β3 hybrid integrins were designed by structure-based sequence alignments. The hybrid α5αv integrin was composed of the α5 domain (amino acids 1–605) fused with the αv domain (amino acids 598–1018), and the hybrid β1β3 integrin consisted of the β1 domain (amino acids 1–459) fused with the β3 domain

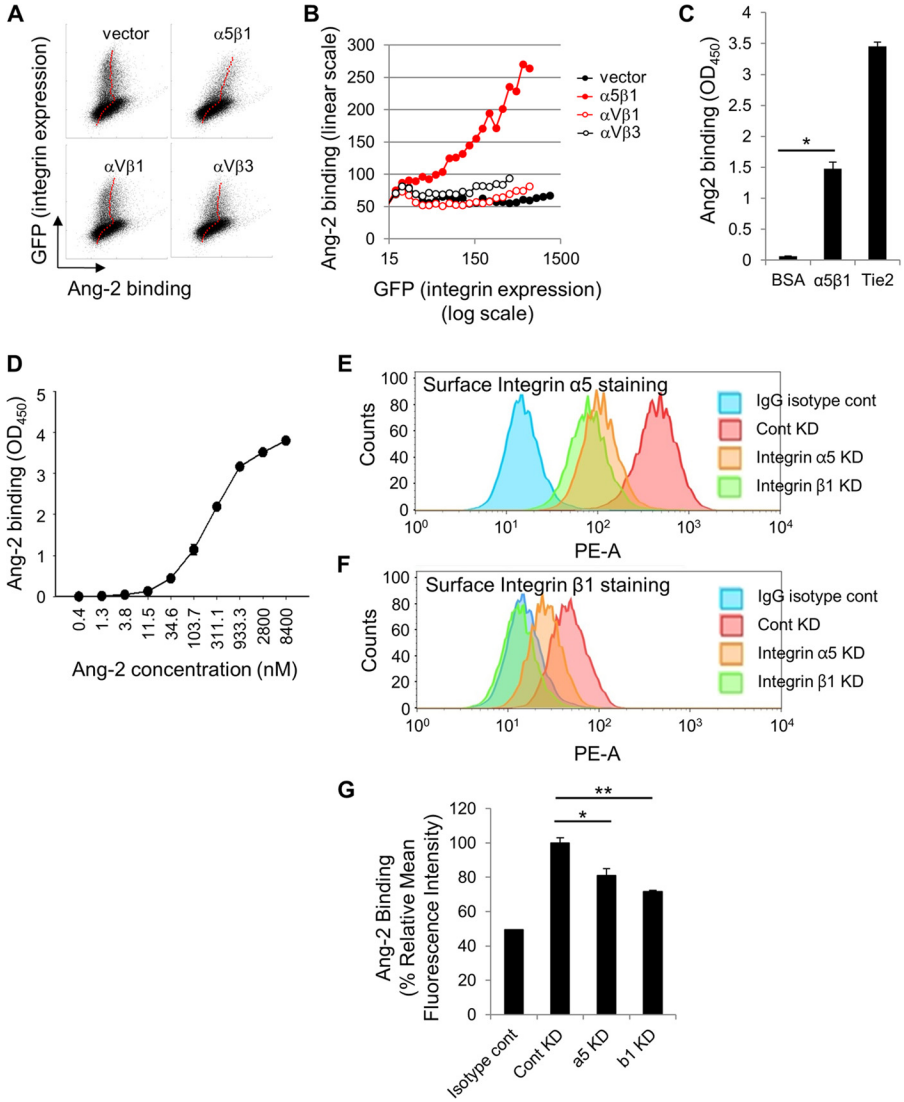

FIGURE 2. **Ang-2 binding to α5β1 integrin.** *A*, CHO cells were cotransfected with integrin cDNAs and GFP cDNA. At 24 h after transfection, the cells were detached, incubated with FLAG-tagged Ang-2, and probed by an anti-FLAG antibody conjugated to phycoerythrin. Fluorescence intensities were analyzed by flow cytometry. Levels of GFP expression (*y* axis) and Ang-2 binding (*x* axis) are depicted as *dot plots*. Geometric mean values of Ang-2 binding in cells expressing different levels of GFP are plotted as *larger red dots*. *B*, levels of Ang-2 binding (*y* axis) and GFP expression (*x* axis) in *A* were plotted as line graphs using the mean values of Ang-2 binding in each range of GFP expression. *C*, FLAG-Ang-2 (10 μg/ml) was incubated in plates coated with 5 μg/ml integrin α5β1, 5 μg/ml Tie2, or BSA. Bound FLAG-Ang-2 was detected using an anti-FLAG antibody conjugated to HRP. The optical density (*OD*) at 450 nm is plotted as a *bar graph*. *Error bars*, S.D. (*, $p < 0.001$). *D*, a quantitative ELISA was performed using a series of diluted concentrations of Ang-2. *E–G*, U87MG cells were transfected with siRNAs targeting α5 or β1 integrin. Reduced expression of integrins on the cell surface was confirmed by flow cytometric analysis of cells transfected with siRNA targeting α5 integrin (*E*) and β1 integrin (*F*). *G*, Ang-2 binding to cells transfected with siRNA targeting integrin α5 or β1 was analyzed by flow cytometry. Mean fluorescence intensities of siRNA-transfected cells were normalized to that of the control siRNA-transfected group. Data are shown as mean ± S.D. (*error bars*) (*, $p < 0.05$; **, $p < 0.01$).

(amino acids 451–762). The hybrid DNA constructs were cloned into the pcDNA3.1 vector (Invitrogen).

Statistical Analyses—Values are presented as mean ± S.D. Statistical differences between means were determined by unpaired Student's *t* test. Statistical significance was set at $p < 0.05$.

RESULTS

Induction of Integrin Signaling by Adhesion of Tie2-negative U87MG Cells to Ang-2—We set out to elucidate the molecular mechanism by identifying which domains are responsible for the binding of Ang-2 to integrins. First, we examined whether Tie2-negative glioma U87MG cells are able to adhere to immobilized Ang-2. A previous study demonstrated by immunoprecipitation that Ang-2 associates with integrins in U87MG cells (10). U87MG cells efficiently adhered to Ang-2-coated plates but not to BSA-coated plates as the negative control (Fig. 1*A*). We confirmed the Tie2 deficiency in U87MG cells by Western blot analysis along with HUVECs as the positive control (Fig. 1*B*). Interestingly, when the cells bound to Ang-2-coated plates, they displayed multiple actin-rich protrusions that were absent when the cells were incubated on poly-L-lysine or fibronectin-coated plates (Fig. 1*C*). Fibronectin, a well known ligand of integrins, was used as the positive control. The Ang-2-dependent actin-rich structures contained vinculin, a well known protein component of integrin-dependent adhesion complexes (Fig. 1*D*). Moreover, cell adhesion to the Ang-2-coated plates

TABLE 1
Sequences of Ang-2 overlapping peptides
The Gln-362 residue is highlighted by boldface type.

1.	^{282}RDCAE VFKSG HTTNG	15.	^{352}EYWLG NEFVS **Q**LTNQ	29.	^{422}DFSTK DGDND KCICK
2.	^{287}VFKSG HTTNG IYTLT	16.	^{357}NEFVS **Q**LTNQ QRYVL	30.	^{428}DGDND KCICK CSQML
3.	^{292}HTTNG IYTLT FPNST	17.	^{362}**Q**LTNQ QRYVL KIHLK	31.	^{432}KCICK CSQML TGGWW
4.	^{297}IYTLT FPNST EEIKA	18.	^{367}QRYVL KIHLK DWEGN	32.	^{437}CSQML TGGWW FDACG
5.	^{302}FPNST EEIKA YCDME	19.	^{372}KIHLK DWEGN EAYSL	33.	^{442}TGGWW FDACG PSNLN
6.	^{307}EEIKA YCDME AGGGG	20.	^{377}DWEGN EAYSL YEHFY	34.	^{447}FDACG PSNLN GMYYP
7.	^{312}YCDME AGGGG WTIIQ	21.	^{382}EAYSL YEHFY LSSEE	35.	^{452}PSNLN GMYYP QRQNT
8.	^{317}AGGGG WTIIQ RREDG	22.	^{387}YEHFY LSSEE LNYRI	36.	^{457}GMYYP QRQNT NKFNG
9.	^{322}WTIIQ RREDG SVDFQ	23.	^{392}LSSEE LNYRI HLKGL	37.	^{462}QRQNT NKFNG IKWYY
10.	^{327}RREDG SVDFQ RTWKE	24.	^{397}LNYRI HLKGL TGTAG	38.	^{467}NKFNG IKWYY WKGSG
11.	^{332}SVDFQ RTWKE YKVGF	25.	^{402}HLKGL TGTAG KISSI	39.	^{472}IKWYY WKGSG YSLKA
12.	^{337}RTWKE YKVGF GNPSG	26.	^{407}TGTAG KISSI SQPGN	40.	^{477}WKGSG YSLKA TTMMI
13.	^{342}YKVGF GNPSG EYWLG	27.	^{412}KISSI SQPGN DFSTK	41.	^{482}YSLKA TTMMI RPADF
14.	^{347}GNPSG EYWLG NEFVS	28.	^{417}SQPGN DFSTK DGDND		

induced Tyr-397 phosphorylation of FAK, a major downstream effector of integrin signaling (Fig. 1*E*). These data were consistent with previous reports using Tie2-negative U87MG and endothelial cells (10, 12). Taken together, these results suggest that Ang-2-mediated cell adhesion leads to the activation of integrin downstream signaling and subsequent protrusion formation in Tie2-negative cells.

Ang-2 Binds to Integrin α5β1—Next, we determined which integrin binds to Ang-2. We focused on α5β1, αvβ1, and αvβ3 integrins that have been suggested to interact with Ang-2 in several reports (9, 10, 12, 13). These reports employed mainly biochemical assays, such as immunoprecipitation and ELISAs, and a cell adhesion assay, where adhesion of target cells to the Ang-2-coated matrix is monitored in the presence of various anti-integrin antibodies. In the present study, in an effort to further characterize the nature and binding domains of the Ang-2/integrin interaction in a more physiologically relevant condition, we employed flow cytometric analysis using integrin-overexpressing cells as a major analysis tool. This procedure allows monitoring of the direct interaction of soluble Ang-2, but not solid matrix-bound Ang-2, with integrins on the cell surface. These integrins were exogenously expressed in CHO cells, together with GFP as a transfection marker.

Using flow cytometric analysis, we first checked the correlation of GFP expression with surface expression of these integrins using anti-β1 or anti-αvβ3 integrin antibodies and confirmed a positive correlation between GFP and integrin expression (data not shown). To exclude any adverse effects of anti-integrin antibodies on the binding of Ang-2 to integrins thereafter, integrin expression was measured indirectly by detecting GFP expression. We found that the expression of α5β1 integrin augmented Ang-2 binding significantly, compared with that of other integrins (Fig. 2, *A* and *B*). Using ELISAs, we further confirmed that Ang-2 interacted with purified α5β1 integrin directly, although the binding strength was weaker than that of the Ang-2/Tie2 interaction (Fig. 2*C*). These data suggest that Ang-2 binds to α5β1 integrin directly with greater affinity than that of other integrins. We then performed a quantitative ELISA using a series of diluted Ang-2 and found that the interaction between Ang2 and α5β1 integrin has a 245 nM equilibrium dissociation constant (K_D) value (Fig. 2*D*).

Furthermore, α5β1 integrin siRNA experiments were carried out, and Ang-2 interaction was examined by flow cytometric analysis. As shown in Fig. 2, *E* and *F*, we confirmed a significant reduction of surface expression of α5 or β1 integrin. Notably, knockdown of either α5 or β1 led to reduced expression of its binding partner, β1 or α5, respectively, indicating that both are needed for stable complex formation and surface expression. We then found that Ang-2 binding to U87MG cells was significantly impaired in α5 or β1 integrin knockdown conditions (Fig. 2*G*), indicating that both endogenous α5 and β1 integrin are necessary for the binding to soluble Ang-2. Taken together, these results point out that Ang-2 binds specifically and directly to α5β1 integrin on the cell surface.

Screening for Inhibitory Peptides to Identify the Integrin-binding Site in Ang-2—We next attempted to define the integrin-binding site in Ang-2 that consists of an N-terminal rod domain for oligomerization and a C-terminal globular fibrinogen-like RBD, which contains three subdomains (the A, B, and P domains) (14). We assumed that the RBD in Ang-2 may be involved in binding to α5β1 integrin because RBDs are interaction modules in various proteins, including fibrinogen.

To identify the integrin-binding domain in Ang-2, we developed a novel cell adhesion assay. We designed 41 overlapping peptides corresponding to the consecutive 15 amino acids within the RBD of Ang-2 with 10 amino acids of each peptide overlapping with those of the neighboring peptide (Table 1). We then tested their inhibitory functions in U87MG cell adhesion onto Ang-2-coated plates. Consistently, peptides 3 (amino acids 292–306), 4 (amino acids 297–311), 15 (amino acids 352–366), and 24 (amino acids 397–411) showed more than 50% inhibition in Ang-2-dependent cell adhesion (Fig. 3*A*), suggesting that the corresponding amino acids in the RBD may be involved in the integrin binding. Interestingly, the identified regions were located on the same side in a three-dimensional model of the Ang-2 RBD (14, 15), indicating the likely integrin

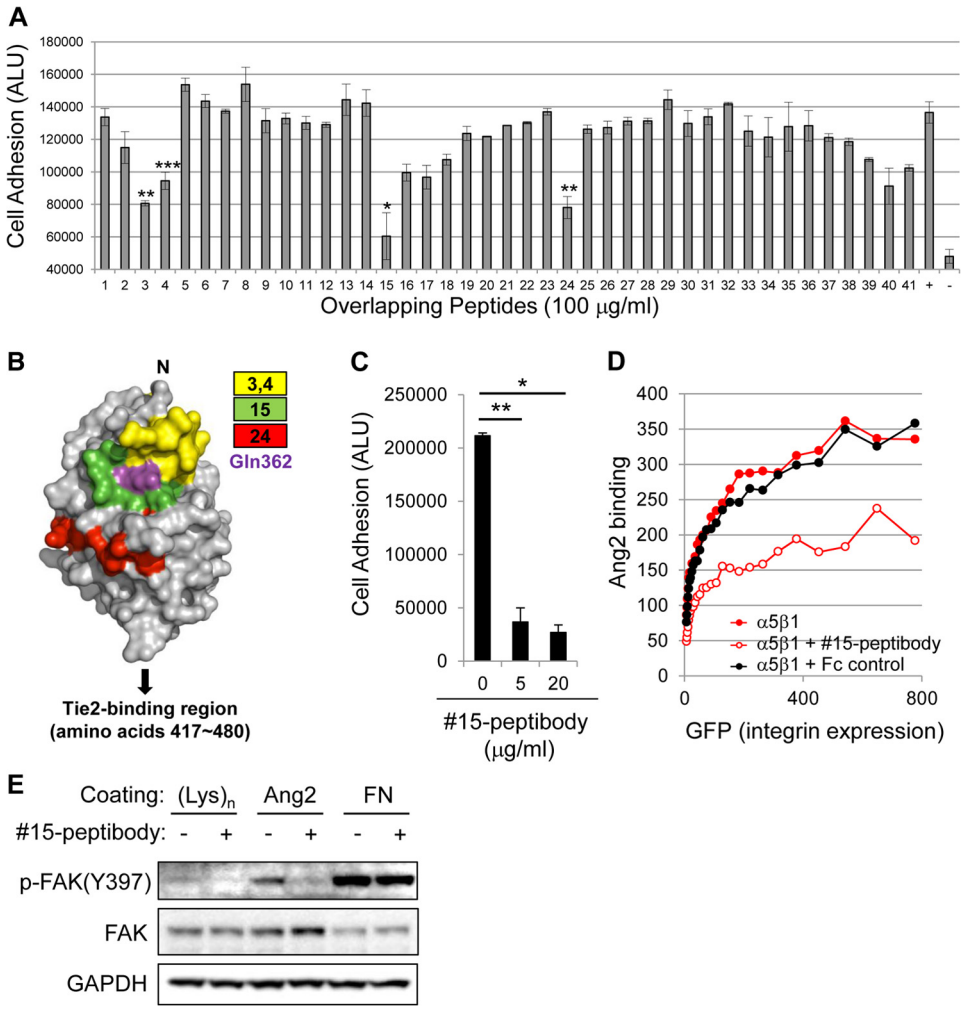

FIGURE 3. **Mapping of integrin-binding sites in Ang-2.** *A*, analysis of Ang-2-dependent U87MG cell adhesion was performed as described in the legend to Fig. 1*A* with the addition of 100 μg/ml of each peptide (Table 1). *ALU*, arbitrary light units. +, positive control without any peptide; −, negative control in which cells were incubated in BSA-coated wells. Note that peptides 3, 4, 15, and 24 showed >50% inhibition of cell adhesion. *Error bars*, S.E. (*, $p < 0.001$; **, $p < 0.01$; ***, $p < 0.05$). *B*, maps of inhibitory peptides on the surface of the Ang-2 RBD using previously reported structural information (Protein Data Bank entry 2GY7) (15). Each peptide is represented by a *different color*. The Gln-362 residue is indicated by *magenta*. *C*, analysis of Ang-2-dependent U87MG cell adhesion was performed in the presence of different doses of 15-peptibody. Data are shown as means ± S.D. (*error bars*) (*, $p < 0.001$; **, $p < 0.01$). *D*, inhibition of the Ang-2-α5β1 integrin interaction by 15-peptibody was examined by flow cytometry. Fc fragment of human IgG was used as a negative control. *E*, the inhibitory effect of 15-peptibody on Ang-2-dependent phosphorylation of FAK at the Tyr-397 site.

binding interface (Fig. 3*B*). Notably, these regions were distinct from the Tie2-binding P domain (amino acids 417–480) of the RBD.

To confirm that the identified regions are important for integrin binding, we chose peptide 15, which was most efficient in the inhibition of Ang-2-dependent cell adhesion, and generated a peptide 15-Fc fusion protein (15-peptibody) in which peptides 15 were fused to both the N and C termini of the Fc portion of a human IgG1 antibody. The 15-peptibody was able to block U87MG cell adhesion to Ang-2 more efficiently than peptide 15, even at a 20-fold lower concentration (Fig. 3*C*), presumably because of an avidity effect resulting from the formation of tetrameric peptides 15 through dimerization of the Fc region. In addition, 15-peptibody blocked Ang-2 binding to CHO cells that overexpress α5β1 integrin (Fig. 3*D*). Finally, 15-peptibody also inhibited the phosphorylation of FAK at Tyr-397 in U87MG cells (Fig. 3*E*). These results clearly show that amino acids 352–366 in Ang-2 (EYWLGNEFVSQLTNQ) are involved in the binding of Ang-2 to α5β1 integrin and regulate the integrin downstream signaling pathway.

Gln-362 in Ang-2 Is Critical for Binding to α5β1 Integrin—To confirm and further map the integrin-binding site in Ang-2, mutational analyses were carried out. Based on the crystal structure of the Ang-2 RBD (Protein Data Bank entry 2GY7) (15), we chose candidate residues as potential binding sites within the amino acid 352–366 region, generated several Ang-2 mutants, and tested their capacity to mediate the binding of Ang-2 to α5β1 integrin in an ELISA. Among them, the Q362E Ang-2 mutant, whose glutamine at the 362 residue is replaced with glutamic acid, was mostly defective in the Ang-2/α5β1 integrin binding assay (data not shown). The Gln-362 residue is located on the surface of one of the α-helices in the RBD (Fig. 3*B*). Under reducing conditions, the Gln-362 Ang-2 mutant and wild-type Ang-2 migrated as a band of the expected molecular mass, ~65 kDa, whereas under non-reducing conditions, both proteins migrated mainly as a dimeric form with ~130

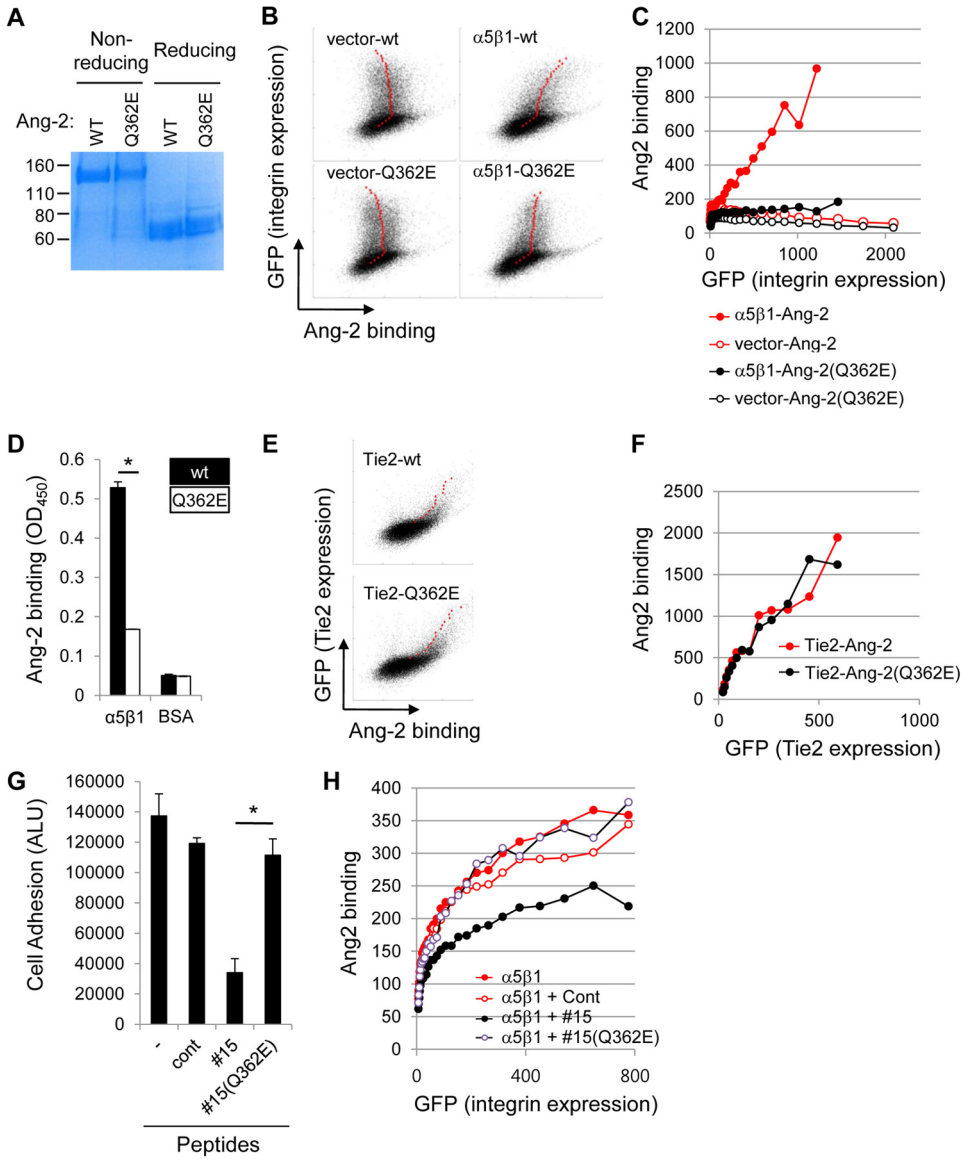

FIGURE 4. **Gln-362 in Ang-2 is essential for binding to integrin α5β1.** *A*, purified recombinant Ang-2 and Q326E Ang-2 proteins were analyzed by SDS-PAGE under non-reducing and reducing conditions. *B*, binding of wild-type or Q362E Ang-2 to integrin-transfected cells was measured by flow cytometry. The Q362E mutation significantly reduced Ang-2 binding to integrin α5β1. *C*, levels of wild-type or Q362E Ang-2 binding to α5β1 integrin (*y* axis) and GFP expression (*x* axis) in *A* were plotted as *line graphs* using the mean values of Ang-2 binding in each range of GFP expression. *D*, effect of the Q362E mutation on the Ang-2-α5β1 integrin interaction was examined by ELISA. Data are shown as means ± S.D. (*, $p < 0.001$). *E*, CHO cells were cotransfected with the Tie2 construct and GFP as a transfection marker. Ang-2 binding to those cells was measured by flow cytometry. *F*, levels of wild-type and Q362E Ang-2 binding to Tie2 (*y* axis) and GFP expression (*x* axis) in *D* were plotted as *line graphs* using the mean values of Ang-2 binding in each range of GFP expression. *G*, analysis of Ang-2-dependent U87MG cell adhesion was performed in the presence of peptide 15 or Q362E mutant of peptide 15 (EYWLGNEFVSELTNQ). A scrambled peptide derived from peptide 15 (*Cont*) was used as a negative control. Data are shown as mean ± S.D. (*error bars*) ($n = 3$; *, $p < 0.001$). *ALU*, arbitrary light units. *H*, interaction between Ang-2 and integrin α5β1 was analyzed by flow cytometry in the presence of peptide 15, the Q362E mutant of peptide 15, or a scrambled peptide (*Cont*).

kDa (Fig. 4*A*), which is consistent with a previous report (16). The Q362E Ang-2 mutant was unable to bind to CHO cells that overexpress α5β1 (Fig. 4, *B* and *C*). In addition, the Q362E mutation also significantly blocked the binding of Ang-2 to purified α5β1 integrin in the ELISA experiment (Fig. 4*D*). However, the Ang-2 Q362E mutant retained the ability to bind to Tie2 (Fig. 4, *E* and *F*). To further confirm that the Gln-362 residue is involved in Ang-2-integrin α5β1 binding, we generated a Q362E mutant version of peptide 15 (EYWLGNEFVSELTNQ) and carried out cell adhesion (Fig. 4*G*) and flow cytometric experiments (Fig. 4*H*). The Q362E mutant of peptide 15 was also unable to inhibit Ang-2 interaction with α5β1 integrin-overexpressing CHO cells. These results demonstrated that the Gln-362 residue in Ang-2 is involved in the interaction with α5β1 integrin but not Tie2.

Gln-362 in Ang-2 Is Essential for Ang-2-mediated Cellular Signaling, Adhesion, and Invasion—Next, we tested the effects of the Q362E Ang-2 mutant on Ang-2-dependent integrin functions in various cells. First, we examined the effect of the Q362E mutation on adhesion of Tie2-deficient U87MG cells that express various integrins, including α5β1 (10). In contrast to wild-type Ang-2, the Q362E Ang-2 mutant lost the adhesive capacity significantly (Fig. 5*A*). In addition, treatment with the Q362E Ang-2 mutant resulted in a dramatic reduction of cell

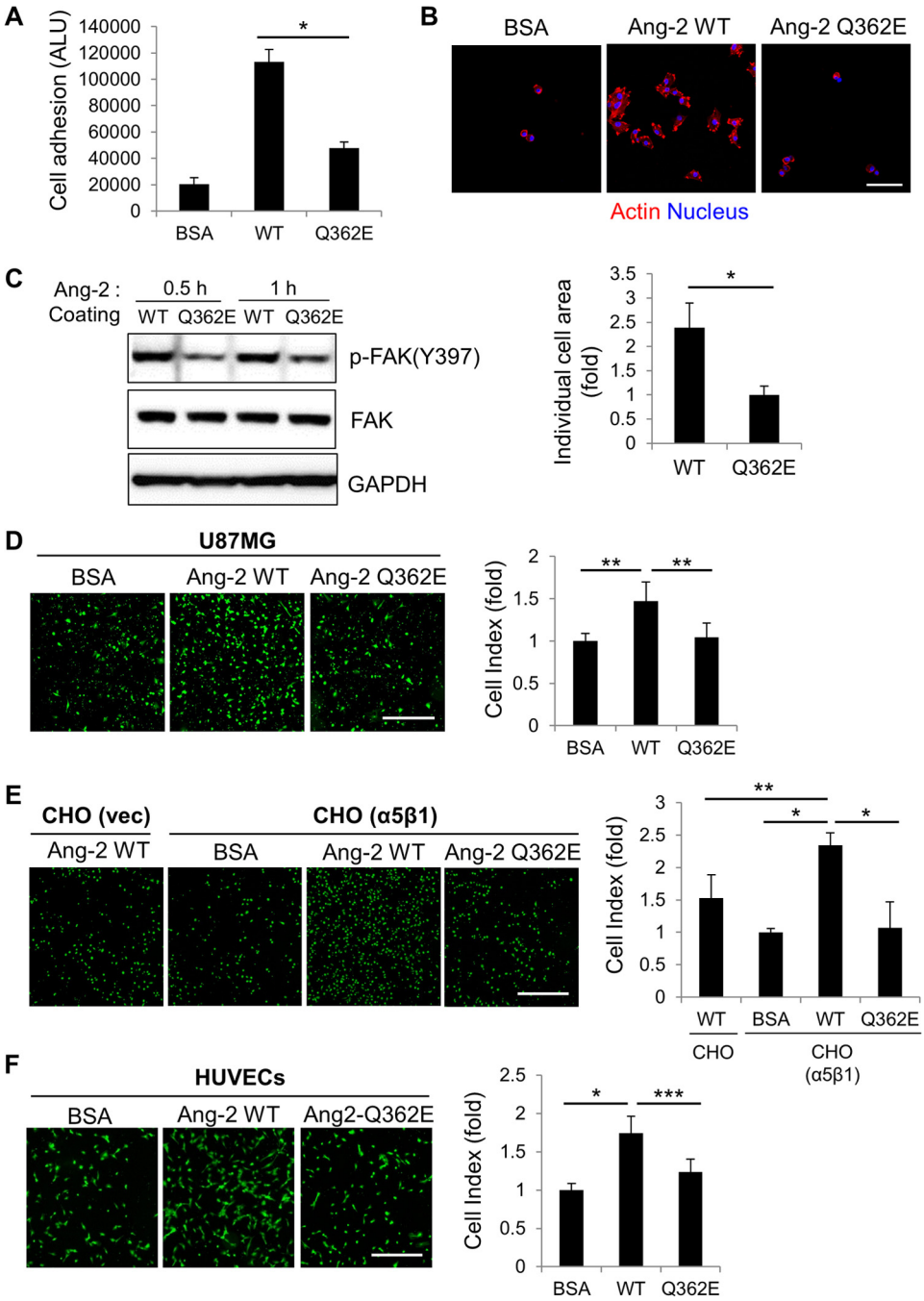

FIGURE 5. **Effects of the Q362E mutation on cell adhesion, signaling, and invasion.** *A*, inhibition of U87MG cell adhesion by the Q362E mutation in Ang-2. Data are shown as means ± S.D. (*error bars*) (*, $p < 0.001$). *ALU*, arbitrary light units. *B*, U87MG cells were seeded on plates coated with Ang-2, Q362E Ang-2, or BSA. After incubation for 2 h, the cells were stained with rhodamine-phalloidin (*red*) and DAPI (*blue*). *Scale bar*, 100 μm. Representative immunofluorescent staining images and quantitative data are shown. The graph represents the mean ± S.D. of the individual cell area that was normalized to the BSA control ($n = 20–30$; *, $p < 0.001$). *C*, effect of the Q362E mutation on Ang-2-dependent FAK phosphorylation. Suspension of serum-starved U87 cells was added into the Ang-2 or Gln-362 Ang-2 mutant-coated culture plates. At 0.5 and 1 h after incubation, cells attached to the plates were harvested and examined by Western analysis. *D–F*, effects of the Q362E mutation on Ang-2-dependent cell invasion were examined in U87MG cells (*D*), α5β1 integrin-transfected CHO cells (*E*), and HUVECs (*F*). Representative images of calcein-labeled invaded cells are shown. *Scale bar*, 500 μm. Quantification of the invaded cells is shown with the mean ± S.D., which was normalized to the BSA control group ($n = 6$; *, $p < 0.01$; **, $p < 0.001$; ***, $p < 0.05$).

spreading and the disappearance of actin-rich protrusions, which was in contrast to the wild-type Ang-2-bound cells (Fig. 5*B*). Furthermore, compared with the cells bound to wild-type Ang-2, those bound to Q362E Ang-2 mutant-coated surfaces displayed a significantly reduced level of phospho-FAK(Tyr-397) (Fig. 5*C*). These results suggest that the Gln-362 in Ang-2 is important not only for binding to integrin α5β1 but also for the activation of integrin downstream signaling and the subsequent cellular responses.

It is well known that cell adhesion and the subsequent protrusion formation by integrin stimulation leads to an increase of cell migration and invasion. Based on these findings, we hypothesized that the Q362E mutation might have a negative influence on cell migration and invasion. To test this hypothe-

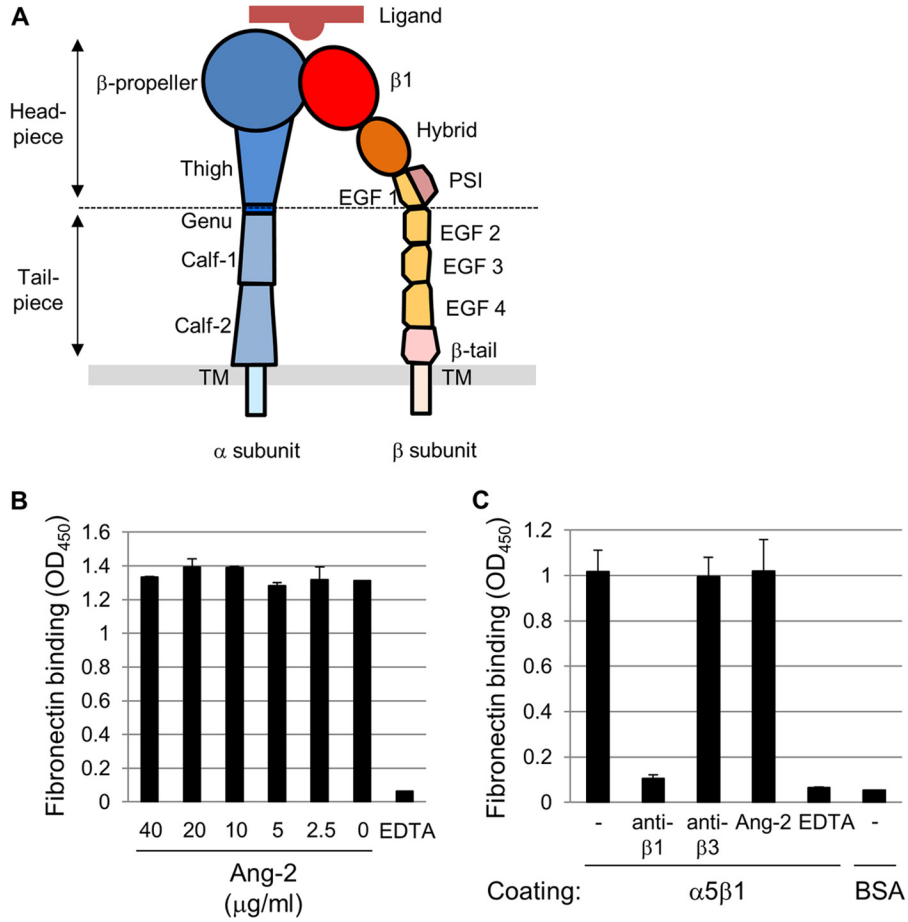

FIGURE 6. **Ang-2 does not compete with fibronectin in binding to α5β1 integrin.** *A*, a schematic diagram of integrin domain structure. The integrin domain structure was adapted and modified from Zhu *et al.* (27). *B*, biotinylated fibronectin (5 μg/ml) was incubated in the presence of increasing amounts of Ang-2 on the plates coated with α5β1 integrin (5 μg/ml). Bound fibronectin was measured in a colorimetric reaction detected by streptavidin conjugated with HRP and TMB. *C*, biotinylated fibronectin was incubated on a α5β1 integrin-coated plate in the presence of 20 μg/ml integrin blocking antibodies, 20 μg/ml Ang2, or 10 mM EDTA. Bound fibronectin was measured as described in *B*.

sis, we carried out a cell invasion assay using wild-type or Q362E Ang-2-coated transwells. Consistent with previous data (10, 17), wild-type Ang-2 significantly stimulated the invasion of Tie2-negative U87MG cells (Fig. 5*D*). In contrast, U87MG cell invasion was significantly inhibited on Q362E Ang-2-coated transwells. We also performed a cell invasion assay using Tie2-deficient CHO cells. Exogenous expression of α5β1 integrin in CHO cells efficiently enhanced cell invasion on wild-type Ang-2-coated plates. However, cell invasion was completely blocked on Q362E Ang-2 mutant-coated plates (Fig. 5*E*). These results suggest that the Gln-362 residue in Ang-2 is critical to induce integrin-mediated migration and invasion of Tie2-deficient cells.

Finally, we determined whether the Ang-2/integrin interaction is also responsible for the invasion of Tie2-expressing HUVECs. Importantly, invasion of HUVECs was significantly inhibited on Q362E Ang-2 mutant-coated transwells (Fig. 5*F*). Because the Q362E mutation does not have any effects on the Ang-2/Tie2 interaction (Fig. 4, *D* and *E*), these results suggest that the Ang-2/integrin interaction is primarily responsible for the migration and invasion of Tie2-positive HUVECs.

Integrin α5 Subunit Mediates the Interaction of Ang-2 and Integrin α5β1—We next attempted to identify the Ang-2 binding region within α5β1 integrin. The head domain interfaces of integrins are common binding sites for the arginine-glycine-aspartic acid (RGD) motif found in diverse extracellular matrix molecules, including fibronectin (Fig. 6*A*) (18). We first tested whether Ang-2 can compete and inhibit the association between fibronectin and α5β1 integrin. Intriguingly, the addition of varying amounts of Ang-2 has no effect on fibronectin binding to α5β1 integrin (Fig. 6*B*). As expected, however, their interaction was completely blocked by either anti-β1 antibody or EDTA treatment (Fig. 6*C*). As a negative control, anti-β3 antibody had no effect. Given that no RGD motif is found in Ang-2, these results suggest that Ang-2 may not compete with fibronectin and potentially bind outside of the head domain in α5β1 integrin.

Based on these findings, we postulated that the binding site for Ang-2 may be located in the tailpiece domain of α5β1 integrin. To test this hypothesis, we generated hybrid constructs in which the tailpiece domains of integrin α5 or β1 were replaced with their equivalents in integrin αv or β3 (referred to as α5αv or β1β3, respectively) (Fig. 7*A*). We then measured their binding capacities by flow cytometric analysis. As shown in Fig. 7*B*, α5αvβ1 integrin with the tailpiece domain of integrin αv displayed a significant reduction in Ang-2 binding capacity. In contrast, α5β1β3 integrin with the tailpiece domain of β3 integrin showed a similar ability for binding to Ang-2, com-

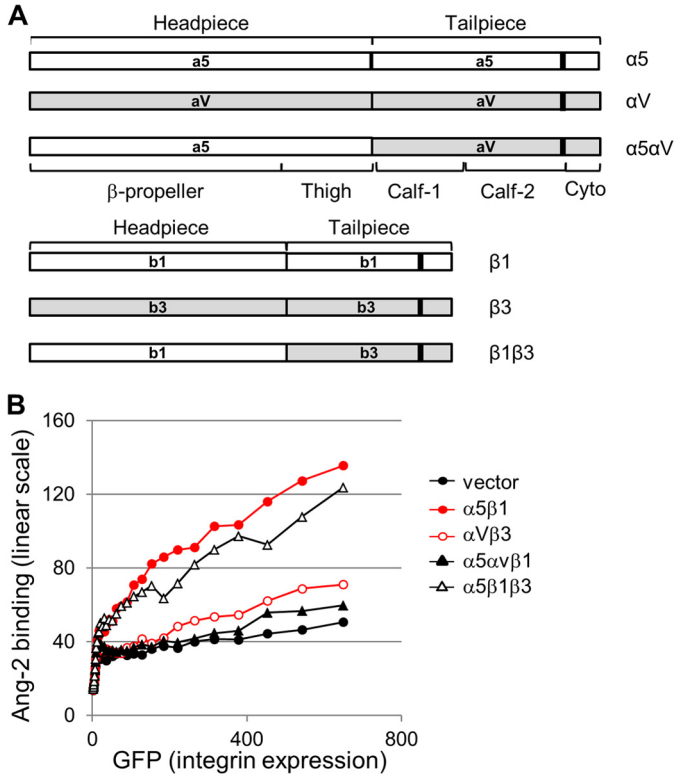

FIGURE 7. **The tailpiece domain of the α5 subunit is essential for binding of α5β1 integrin to Ang-2.** *A*, domain structures of the integrin hybrid constructs for α5αvβ1 and α5β1β3. *B*, CHO cells transfected with the indicated integrin construct and GFP as a transfection marker were tested for their Ang-2 binding capacity. Levels of Ang-2 binding to integrins (*y* axis) and GFP expression (*x* axis) were plotted as *line graphs* using the mean values of Ang-2 binding in each range of GFP expression.

pared with the interaction of wild-type α5β1 integrin and Ang-2. Taken together, these data suggest that the tailpiece domain of the α5 subunit plays a key role in the binding of α5β1 integrin to Ang-2.

DISCUSSION

The function of Ang-2 in angiogenesis and tumor metastasis is mediated by interaction with several integrins as well as the well known endothelial cell receptor Tie2. Although the key structural residues responsible for Ang-2/Tie2 interaction were determined (15), the binding domains in the Ang-2/integrin interaction remain unidentified. By utilizing a systematic screening method using Ang-2-derived peptides and diverse biochemistry/cell-based analyses, the present study demonstrates that the Gln-362 residue of Ang-2 and the tailpiece domain of the integrin α5 subunit are involved in Ang-2/α5β1 integrin interaction and subsequent cellular signaling. The results suggest that the Ang-2 Gln-362 residue plays a key role in the agonistic action of Ang-2 to regulate cell invasion by regulating integrin functions in both Tie2-negative tumor and endothelial cells.

The present study and other previous studies consistently demonstrated that Ang-2 can bind to various integrins. However, the affinity strength between Ang-2 and integrins has been reported to be varied, depending on the assays used. In this study, we showed that α5β1 integrin has stronger affinity toward Ang-2 than αvβ1 and αvβ3 integrins in flow cytometric analysis (Fig. 2). A recent study, however, showed that α3β1, αvβ3, αvβ5, and α5β1 integrins have comparable affinities toward Ang-2 in immunoprecipitation, ELISAs, and Ang-2-mediated cell adhesion assays using Ang-2-coated plates (12). Considering that Ang-2 tends to aggregate easily and exists in heterogeneous, multimeric forms, this difference may arise from the possibility that the solid matrix-coated Ang-2 and the soluble Ang-2 used in flow cytometic analysis may exist in different status, affecting the binding affinity to integrins. However, we also cannot exclude the possibility that Ang-2 may have stronger affinity toward other integrins, which were not included in this study.

By carrying out systematic cell adhesion assays using 41 peptides with sequences originating from the RBD of Ang-2, we successfully identified several peptides that blocked the binding of Ang-2 to Tie2-negative, integrin-positive cells and established the Gln-362 of Ang-2 as a critical residue for integrin binding but not Tie2 binding (Fig. 4). Gln-362 is exposed in the α3-helical groove area of the B domain in the RBD (14), which is separate from the Tie2-binding region in the P domain of the Ang-2 RBD (15). These results indicate that Ang-2 may use different regions for binding to its distinct partners. We propose a model in which a middle large B domain containing Gln-362 in the Ang-2 RBD is involved in binding to integrins (Fig. 3*B*). Further study is necessary to test whether the Gln-362 residue and the B domain of Ang-2 are also involved in interaction with other integrins. In the future, it would be also important to examine whether any structural changes in integrins occur upon their association, which may contribute to the activation of integrin downstream signaling and subsequent cellular responses.

Several integrins, including α5β1, show both RGD-dependent and RGD-independent binding capacity. The RGD-containing ligands, including fibronectin and vitronectin, bind to the head domain interface between the α and β subunits in integrins (18). A recent report suggested that the β I-like domain of integrins in its high affinity conformation is likely to be involved in interaction with Ang-2, based on the data showing that treatment with cations inhibited Ang-2/integrin interaction. However, the direct interaction between Ang-2 and the β1 subunit has not yet been demonstrated (12). To the best of our knowledge, the present study is the first report showing that an integrin binder can associate with the tailpiece domain of integrin. In this sense, Ang-2 seems to have a very unusual mode of action as an integrin ligand. Although tetraspanin (CD151) can bind to the tailpiece domain of integrins, its interaction appears to potentiate the ligand binding activity of integrin α3β1 by stabilizing its active conformation (19). Considering the multimeric nature of Ang-2, it would be interesting to examine whether Ang-2 can activate integrin signaling by inducing integrin clustering and boost extracellular matrix-induced integrin signaling without perturbation of the integrin-extracellular matrix interaction.

Several therapeutic Ang2 antibodies are being tested in clinical trials in diverse cancer patients (20–22), with the main paradigm that cancer patients may benefit from Ang2 antibodies that interfere with the interaction between Ang-2 and Tie2, thus regressing tumor angiogenesis. Those antibodies whose

epitopes are mainly located in the Tie2-binding P domain of Ang-2 (amino acids 417–480) were selected for their superior ability to inhibit Ang-2/Tie2 association in the endothelial cell-based assay (23). In this study, we propose that Ang-2 antibodies that can inhibit the interaction between Ang-2 and integrins may also have an anti-tumor effect by inhibiting tumor invasion/metastasis, and the B domain of Ang-2 RBD may be considered as a target in the development of anti-Ang2 antibodies. It would be worthwhile to investigate whether those Ang-2 antibodies in the clinical trials can inhibit the interaction between Ang-2 and integrins.

In summary, the present study provides a novel mechanistic insight and provides detailed information about the binding domains of the Ang-2/integrin α5β1 interaction. The strong correlation of Ang-2 expression and the invasion and metastasis of various cancers (9, 24, 25) and α5β1 integrin expression in diverse human cancers (26) underscores the significance of integrin and Ang-2 interactions in cancer progression. The present study suggests a novel therapeutic approach in cancer treatment by blockade of Ang-2/integrin interaction.

Acknowledgment—We thank Christina Yi for valuable advice and editing of the manuscript.

REFERENCES

1. Augustin, H. G., Koh, G. Y., Thurston, G., and Alitalo, K. (2009) Control of vascular morphogenesis and homeostasis through the angiopoietin-Tie system. *Nat. Rev. Mol. Cell Biol.* **10,** 165–177
2. Chung, A. S., Lee, J., and Ferrara, N. (2010) Targeting the tumour vasculature: insights from physiological angiogenesis. *Nat. Rev. Cancer* **10,** 505–514
3. Lewis, C. E., and Ferrara, N. (2011) Multiple effects of angiopoietin-2 blockade on tumors. *Cancer Cell* **19,** 431–433
4. Eklund, L., and Saharinen, P. (2013) Angiopoietin signaling in the vasculature. *Exp. Cell Res.* **319,** 1271–1280
5. Daly, C., Eichten, A., Castanaro, C., Pasnikowski, E., Adler, A., Lalani, A. S., Papadopoulos, N., Kyle, A. H., Minchinton, A. I., Yancopoulos, G. D., and Thurston, G. (2013) Angiopoietin-2 functions as a Tie2 agonist in tumor models, where it limits the effects of VEGF inhibition. *Cancer Res.* **73,** 108–118
6. Gale, N. W., Thurston, G., Hackett, S. F., Renard, R., Wang, Q., McClain, J., Martin, C., Witte, C., Witte, M. H., Jackson, D., Suri, C., Campochiaro, P. A., Wiegand, S. J., and Yancopoulos, G. D. (2002) Angiopoietin-2 is required for postnatal angiogenesis and lymphatic patterning, and only the latter role is rescued by angiopoietin-1. *Dev. Cell* **3,** 411–423
7. Thomas, M., Felcht, M., Kruse, K., Kretschmer, S., Deppermann, C., Biesdorf, A., Rohr, K., Benest, A. V., Fiedler, U., and Augustin, H. G. (2010) Angiopoietin-2 stimulation of endothelial cells induces αvβ3 integrin internalization and degradation. *J. Biol. Chem.* **285,** 23842–23849
8. Cascone, I., Napione, L., Maniero, F., Serini, G., and Bussolino, F. (2005) Stable interaction between α5β1 integrin and Tie2 tyrosine kinase receptor regulates endothelial cell response to Ang-1. *J. Cell Biol.* **170,** 993–1004
9. Imanishi, Y., Hu, B., Jarzynka, M. J., Guo, P., Elishaev, E., Bar-Joseph, I., and Cheng, S. Y. (2007) Angiopoietin-2 stimulates breast cancer metastasis through the $\alpha_5\beta_1$ integrin-mediated pathway. *Cancer Res.* **67,** 4254–4263
10. Hu, B., Jarzynka, M. J., Guo, P., Imanishi, Y., Schlaepfer, D. D., and Cheng, S. Y. (2006) Angiopoietin 2 induces glioma cell invasion by stimulating matrix metalloprotease 2 expression through the αvβ1 integrin and focal adhesion kinase signaling pathway. *Cancer Res.* **66,** 775–783
11. Imanishi, Y., Hu, B., Xiao, G., Yao, X., and Cheng, S. Y. (2011) Angiopoietin-2, an angiogenic regulator, promotes initial growth and survival of breast cancer metastases to the lung through the integrin-linked kinase (ILK)-AKT-B cell lymphoma 2 (Bcl-2) pathway. *J. Biol. Chem.* **286,** 29249–29260
12. Felcht, M., Luck, R., Schering, A., Seidel, P., Srivastava, K., Hu, J., Bartol, A., Kienast, Y., Vettel, C., Loos, E. K., Kutschera, S., Bartels, S., Appak, S., Besemfelder, E., Terhardt, D., Chavakis, E., Wieland, T., Klein, C., Thomas, M., Uemura, A., Goerdt, S., and Augustin, H. G. (2012) Angiopoietin-2 differentially regulates angiogenesis through TIE2 and integrin signaling. *J. Clin. Invest.* **122,** 1991–2005
13. Carlson, T. R., Feng, Y., Maisonpierre, P. C., Mrksich, M., and Morla, A. O. (2001) Direct cell adhesion to the angiopoietins mediated by integrins. *J. Biol. Chem.* **276,** 26516–26525
14. Barton, W. A., Tzvetkova, D., and Nikolov, D. B. (2005) Structure of the angiopoietin-2 receptor binding domain and identification of surfaces involved in Tie2 recognition. *Structure* **13,** 825–832
15. Barton, W. A., Tzvetkova-Robev, D., Miranda, E. P., Kolev, M. V., Rajashankar, K. R., Himanen, J. P., and Nikolov, D. B. (2006) Crystal structures of the Tie2 receptor ectodomain and the angiopoietin-2-Tie2 complex. *Nat. Struct. Mol. Biol.* **13,** 524–532
16. Kim, H., Jung, K., Kim, H. M., Cheng, Y., and Koh, G. Y., (2009) A designed angiopoietin-2 variant, pentameric COMP-Ang2, strongly activates Tie2 receptor and stimulates angiogenesis. *Biochim. Biophys. Acta* **1793,** 772–780
17. Hu, B., Guo, P., Fang, Q., Tao, H.-Q., Wang, D., Nagane, M., Su Huang, H.-J., Gunji, Y., Nishikawa, R., Alitalo, K., Cavenee, W. K., and Cheng, S.-Y. (2003) Angiopoietin-2 induces human glioma invasion through the activation of matrix metalloprotease-2. *Proc. Natl. Acad. Sci. U.S.A.* **100,** 8904–8909
18. Xiong, J.-P., Stehle, T., Zhang, R., Joachimiak, A., Frech, M., Goodman, S. L., and Arnaout, M. A. (2002) Crystal structure of the extracellular segment of integrin αvβ3 in complex with an Arg-Gly-Asp ligand. *Science* **296,** 151–155
19. Nishiuchi, R., Sanzen, N., Nada, S., Sumida, Y., Wada, Y., Okada, M., Takagi, J., Hasegawa, H., and Sekiguchi, K. (2005) Potentiation of the ligand-binding activity of integrin α3β1 via association with tetraspanin CD151. *Proc. Natl. Acad. Sci. U.S.A.* **102,** 1939–1944
20. Leow, C. C., Coffman, K., Inigo, I., Breen, S., Czapiga, M., Soukharev, S., Gingles, N., Peterson, N., Fazenbaker, C., Woods, R., Jallal, B., Ricketts, S. A., Lavallee, T., Coats, S., and Chang, Y. (2012) MEDI3617, a human anti-angiopoietin 2 monoclonal antibody, inhibits angiogenesis and tumor growth in human tumor xenograft models. *Int. J. Oncol.* **40,** 1321–1330
21. Gerald, D., Chintharlapalli, S., Augustin, H. G., and Benjamin, L. E. (2013) Angiopoietin-2: an attractive target for improved antiangiogenic tumor therapy. *Cancer Res.* **73,** 1649–1657
22. Cascone, T., and Heymach, J. V. (2012) Targeting the angiopoietin/Tie2 pathway: cutting tumor vessels with a double-edged sword? *J. Clin. Oncol.* **30,** 441–444
23. Thurston, G., and Daly, C. (February 3, 2011) High Affinity Human Antibodies to Human Angiopoietin-2. Regeneron Pharmaceuticals, Inc., United States Patent US2011/0027286A1
24. Sfiligoi, C., de Luca, A., Cascone, I., Sorbello, V., Fuso, L., Ponzone, R., Biglia, N., Audero, E., Arisio, R., Bussolino, F., Sismondi, P., and De Bortoli, M. (2003) Angiopoietin-2 expression in breast cancer correlates with lymph node invasion and short survival. *Int. J. Cancer* **103,** 466–474
25. Schulz, P., Fischer, C., Detjen, K. M., Rieke, S., Hilfenhaus, G., von Marschall, Z., Böhmig, M., Koch, I., Kehrberger, J., Hauff, P., Thierauch, K. H., Alves, F., Wiedenmann, B., and Scholz, A. (2011) Angiopoietin-2 drives lymphatic metastasis of pancreatic cancer. *FASEB J.* **25,** 3325–3335
26. Desgrosellier, J. S., and Cheresh, D. A. (2010) Integrins in cancer: biological implications and therapeutic opportunities. *Nat. Rev. Cancer* **10,** 9–22
27. Zhu, J., Zhu, J., and Springer, T. A. (2013) Complete integrin headpiece opening in eight steps. *J. Cell Biol.* **201,** 1053–1068